

ades of life<sup>(6,7)</sup>, with a slight predilection for males and preferential involvement of the sacrococcygeal region (50%), followed by the sphenoccipital region (35%), cervical spine, and lumbar spine, occurring only rarely in the dorsal spine and posterior mediastinum<sup>(6-8)</sup>. Symptoms often appear only after the lesion has reached large proportions, with local invasion affecting neurovascular structures. Local recurrence is common when complete resection was not possible.

The differential diagnoses of chordoma include metastases, chondrosarcoma, multiple myeloma, neurogenic tumors, among others. Although imaging methods help delineate the lesion, the diagnosis is made on the basis of the histopathological analysis<sup>(7)</sup>.

On MRI, most chordomas show isointense or hypointense signals in T1-weighted sequences, whereas they show hyperintense signals in T2-weighted and short-tau inversion-recovery sequences, reflecting their high water content, some lesions containing fibrous septa and therefore showing low signal intensity in T2-weighted sequences<sup>(6-8)</sup>. Gadolinium contrast enhancement tends to be moderate and heterogeneous<sup>(6,8)</sup>. Lesions are often accompanied by bone erosion, which was not observed in the case reported here. Recent studies have highlighted the use of diffusion-weighted imaging in the differentiation between chordomas and chondrosarcomas, reporting that the latter show higher apparent diffusion coefficients<sup>(9,10)</sup>.

In addition to an unusual site of involvement, our patient presented the peculiarity of a synchronous lesion. Although some authors have reported similar cases<sup>(7,8,11,12)</sup>, there is no specific criterion for differentiating between a multicentric chordoma and metastatic dissemination. We believe that our case could represent dissemination to the cerebrospinal fluid, because there was involvement of the vertebral canal.

The treatment of choice for chordoma is surgical resection with adjuvant radiotherapy, resulting in a disease-free period approximately 2.5 years longer than that achieved after surgical treatment alone<sup>(7)</sup>. Because chordoma is resistant to conventional radiotherapy, other modalities, such as stereotactic radiosurgery, are used. Chordoma does not respond well to chemotherapy, antitumor activity having been observed, in small studies, only with the use of imatinib mesylate<sup>(13)</sup>.

Albeit rare, a diagnosis of chordoma should be considered in patients with lesions affecting the posterior mediastinum. In

addition, the possibility of synchronous lesions should be investigated in such patients.

#### REFERENCES

- Guimaraes MD, Hochegger B, Koenigkam-Santos M, et al. Magnetic resonance imaging of the chest in the evaluation of cancer patients: state of the art. *Radiol Bras.* 2015;48:33–42.
- Pessanha LB, Melo AMF, Braga FS, et al. Acute post-tonsillectomy negative pressure pulmonary edema. *Radiol Bras.* 2015;48:197–8.
- Barbosa BC, Marchiori E, Zanetti G, et al. Catamenial pneumothorax. *Radiol Bras.* 2015;48:128–9.
- Nishiyama KH, Falcão EAA, Kay FU, et al. Acute tracheobronchitis caused by *Aspergillus*: case report and imaging findings. *Radiol Bras.* 2014;47:317–9.
- Fernandes GL, Teixeira AA, Antón AGS, et al. Churg-Strauss syndrome: a case report. *Radiol Bras.* 2014;47:259–61.
- Rodallec MH, Feydy A, Larousserie F, et al. Diagnostic imaging of solitary tumors of the spine: what to do and say. *Radiographics.* 2008;28:1019–41.
- Aydin AL, Sasani M, Oktenoglu T, et al. A case of chordoma invading multiple neuroaxial bones: report of ten years follow up. *Turk Neurosurg.* 2013;23:551–6.
- Lim JJ, Kim SH, Cho KH, et al. Chordomas involving multiple neuraxial bones. *J Korean Neurosurg Soc.* 2009;45:35–8.
- Yeom KW, Lober RM, Mobley BC, et al. Diffusion-weighted MRI: distinction of skull base chordoma from chondrosarcoma. *AJNR Am J Neuroradiol.* 2013;34:1056–61.
- Freeze BS, Glastonbury CM. Differentiation of skull base chordomas from chondrosarcomas by diffusion-weighted MRI. *AJNR Am J Neuroradiol.* 2013;34:E113.
- Badwal S, Pal L, Basu A, et al. Multiple synchronous spinal extraosseous intradural chordomas: is it a distinct entity? *Br J Neurosurg.* 2006;20:99–103.
- Simon SL, Inneh IA, Mok CL, et al. Multiple epidural lumbar chordomas without bone involvement in a 17-year-old female: a case report. *Spine J.* 2011;11:e7–10.
- Casali PG, Stacchiotti S, Sangalli C, et al. Chordoma. *Curr Opin Oncol.* 2007;19:367–70.

#### Bruno Niemeyer de Freitas Ribeiro<sup>1</sup>, Edson Marchiori<sup>2</sup>

- Instituto Estadual do Cérebro Paulo Niemeyer, Rio de Janeiro RJ, Brazil.
- Universidade Federal do Rio de Janeiro (UFRJ), Rio de Janeiro, RJ, Brazil. Mailing address: Dr. Bruno Niemeyer de Freitas Ribeiro. Instituto Estadual do Cérebro Paulo Niemeyer – Departamento de Radiologia. Rua do Rezende, 156, Centro. Rio de Janeiro, RJ, Brazil, 20231-092. E-mail: bruno.niemeyer@hotmail.com.

<http://dx.doi.org/10.1590/0100-3984.2016.0059>

#### Esthesioneuroblastoma

Dear Editor,

A 64-year-old male presented with nasal obstruction, anosmia, and a reduction in visual acuity over the last few months, together with weight loss and a two-year history of headache. Computed tomography (CT) of the brain (Figure 1A) showed an expansile lesion with poorly defined borders, occupying the ethmoid cells, sphenoid sinuses, and the anterior cranial fossa, accompanied by edema of the frontal lobes. On magnetic resonance imaging (MRI) scans (Figures 1B, 1C, and 1D), the lesion showed restricted diffusion and intense enhancement after contrast administration. A biopsy was performed, and analysis of the biopsy sample revealed hyperchromatic cells organized around a fibrillar stroma, forming rosettes, consistent with a diagnosis of olfactory neuroblastoma. The lesion was staged histologically as grade I in the Hyams grading system. There was no evidence of cervical involvement or distant metastases. The patient died 15 days after undergoing the examinations.

Olfactory neuroblastoma, also known as esthesioneuroblastoma, is a rare malignant neoplasm of neuroectodermal origin and accounts for 3–6% of all malignant tumors of the paranasal sinuses. It has a bimodal age distribution, being most common among adults in the second or fifth decades of life<sup>(1)</sup>. It is believed that the neoplasm arises from the olfactory epithelium, originating in the superior portion of the nasal cavities, ascending across the cribriform plate, and extending into the anterior cranial fossa<sup>(2)</sup>.

Clinically, olfactory neuroblastoma manifests as nasal obstruction or epistaxis. It can show indolent behavior, promote local invasion, and generate distant metastases. It tends to invade the paranasal sinuses, orbits, and anterior cranial fossa. The most common metastases are to the lymph nodes of the neck, lungs, liver, and bone, such dissemination at the time of diagnosis being the main predictor of survival<sup>(2)</sup>. Although there is no universally accepted staging system, the Kadish classification system, established in 1976 and considered an important prognostic predictor, is widely used. In the Kadish system, stage

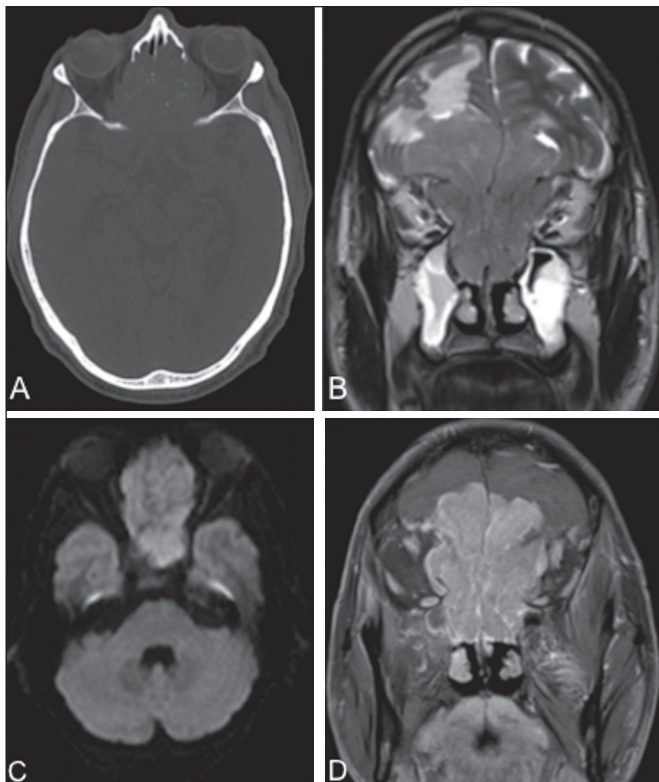


**Figure 1.** CT of the brain (A), with a bone window, showing an expansile lesion occupying ethmoid cells and containing calcifications, with bone destruction. MRI demonstrated that the lesion was extra-axial, with lobulated contours, located in the upper portion of the nasal cavity, and extended to the anterior cranial fossa, facial sinuses, and orbits. A coronal T2-weighted sequence (B) shows that the expansile lesion presented an isointense signal, although a hyperintense signal (edema) can be seen in the brain parenchyma in the frontal lobe, mainly on the left. An axial diffusion-weighted imaging sequence (C) shows a hyperintense signal (restricted diffusion). A contrast-enhanced coronal T1-weighted sequence (D) shows intense enhancement.

A indicates that the tumor is limited to the nasal cavity; stage B indicates that it involves only the nasal cavity and paranasal sinuses; and stage C indicates that it extends beyond the stage B limits. The staging system proposed by Dulguerov employs the tumor-node-metastasis classification<sup>(3,4)</sup>.

Bone destruction and calcification within the lesion can be characterized by CT<sup>(5)</sup>. An MRI scan provides more accurate information on the extent of the tumor, especially in terms of intracranial and orbital involvement. On MRI, the majority of olfactory neuroblastomas present a signal that is (in relation to that of muscle tissue) hypointense in T1-weighted sequences

and hyperintense in T2-weighted sequences, as well as showing intense enhancement in contrast-enhanced sequences<sup>(6,7)</sup>. MRI is also superior to CT in the evaluation of recurrence after craniofacial resection, because of its greater ability to differentiate fibrous scar tissue from residual or recurring neoplasia<sup>(6)</sup>. Cysts in the intracranial margin of the tumor have been reported in cases of olfactory neuroblastoma. Another relevant aspect is a dumbbell-like morphology, the tumor mass being divided between the anterior cranial fossa and the nasal cavity, the cribriform plate forming the “waist”<sup>(5)</sup>.

The main differential diagnoses of olfactory neuroblastoma include: squamous cell carcinoma, typically in the maxillary antrum, with bone erosion; sinonasal adenocarcinoma, with heterogeneous enhancement, which has been associated with occupational exposure to wood dust; undifferentiated sinonasal carcinoma, which affects older patients; and dural-based invasive meningioma, with poorly defined borders and areas of necrosis<sup>(8)</sup>.

#### REFERENCES

1. Ferreira MCF, Tonoli C, Varoni ACC, et al. Estesioneuroblastoma. *Rev Ciênc Méd.* 2007;16:193–8.
2. Howell MC, Branstetter BF 4th, Snyderman CH. Patterns of regional spread for esthesioneuroblastoma. *AJNR Am J Neuroradiol.* 2011;32:929–33.
3. Van Gompel JJ, Giannini C, Olsen KD, et al. Long-term outcome of esthesioneuroblastoma: Hyams grade predicts patient survival. *J Neuro Surg B Skull Base.* 2012;73:331–6.
4. Tajudeen BA, Arshi A, Suh JD, et al. Importance of tumor grade in esthesioneuroblastoma survival: a population-based analysis. *JAMA Otolaryngol Head Neck Surg.* 2014;140:1124–9.
5. Mendonça VF, Carvalho ACP, Freitas E, et al. Tumores malignos da cavidade nasal: avaliação por tomografia computadorizada. *Radiol Bras.* 2005;38:175–80.
6. Li C, Yousem DM, Hayden RE, et al. Olfactory neuroblastoma: MR evaluation. *AJNR Am J Neuroradiol.* 1993;14:1167–71.
7. Schuster JJ, Phillips CD, Levine PA. MR of esthesioneuroblastoma (olfactory neuroblastoma) and appearance after craniofacial resection. *AJNR Am J Neuroradiol.* 1994;15:1169–77.
8. Baptista AC, Marchiori E, Boasquevisque E, et al. Comprometimento órbito-craniano por tumores malignos sinonasais: estudo por tomografia computadorizada. *Radiol Bras.* 2002;35:277–85.

**Aline de Araújo Naves<sup>1</sup>, Luiz Gonzaga da Silveira Filho<sup>1</sup>, Renata Etchebehere<sup>1</sup>, Hélio Antônio Ribeiro Júnior<sup>2</sup>, Francisco Valtener A. Lima Junior<sup>2</sup>**

1. Universidade Federal do Triângulo Mineiro (UFTM), Uberaba, MG, Brazil.
2. Hospital das Clínicas da Faculdade de Medicina de Ribeirão Preto da Universidade de São Paulo (HCFMRP-USP), Ribeirão Preto, SP, Brazil. Mailing address: Dra. Aline de Araújo Naves. Universidade Federal do Triângulo Mineiro. Avenida Getúlio Guaritá, 130, Nossa Senhora da Abadia. Uberaba, MG, Brazil, 38025-440. E-mail: rdi.alinenaves@gmail.com.

<http://dx.doi.org/10.1590/0100-3984.2015.0206>

#### Giant ovarian teratoma: an important differential diagnosis of pelvic masses in children

Dear Editor,

An 8-year-old female patient presented with diffuse abdominal pain accompanied by progressive distension. Physical examination revealed a large abdominal mass, predominantly in the mesogastrium, that was depressible and painless on palpation. Ultrasound showed a solid-cystic formation extending from the epigastrium to the hypogastrium, with a calcium component and an air-fluid level (Figure 1). Computed tomography (CT) showed a massive solid-cystic formation, with a fat component and soft tissue, as well as calcifications, measuring 12.6 × 19.2

× 20.8 cm, exerting a significant mass effect, displacing the small intestine, aorta, and inferior vena cava, as well as causing slight compression of the pancreas, kidneys, and ureters, with no apparent signs of infiltration (Figure 2). Intraoperatively, the mass was seen to be adhered to the left fallopian tube and to the greater omentum (Figure 1). The tumor was excised without complications, and the patient was discharged five days later. A follow-up abdominal ultrasound revealed no changes.

The occurrence of an abdominal mass in a child should always be evaluated by a pediatrician. The main differential diagnoses are organomegaly and fecal impaction. When abdominal palpation produces nonspecific findings, further investigation, employing imaging methods, is required<sup>(1)</sup>.